Title
Conformational selectivity in cytochrome P450 redox partner interactions

Journal
Proceedings of the National Academy of Sciences of the United States of America, 113(31)

ISSN
0027-8424

Authors
Hollingsworth, Scott A
Batabyal, Dipanwita
Nguyen, Brian D
et al.

Publication Date
2016-08-02

DOI
10.1073/pnas.1606474113

Peer reviewed

Conformational selectivity in cytochrome P450 redox partner interactions

Scott A. Hollingsworth[a,b,c,1], Dipanwita Batabyal[a,b,c,1], Brian D. Nguyen[a,b,c], and Thomas L. Poulos[a,b,c,2]

[a]Department of Molecular Biology and Biochemistry, University of California, Irvine, CA 92697; [b]Department of Pharmaceutical Sciences, University of California, Irvine, CA 92697; and [c]Department of Chemistry, University of California, Irvine, CA 92697

Edited by Ken A. Dill, Stony Brook University, Stony Brook, NY, and approved June 8, 2016 (received for review April 22, 2016)

The heme iron of cytochromes P450 must be reduced to bind and activate molecular oxygen for substrate oxidation. Reducing equivalents are derived from a redox partner, which requires the formation of a protein–protein complex. A subject of increasing discussion is the role that redox partner binding plays, if any, in favoring significant structural changes in the P450s that are required for activity. Many P450s now have been shown to experience large open and closed motions. Several structural and spectral studies indicate that the well-studied P450cam adopts the open conformation when its redox partner, putidaredoxin (Pdx), binds, whereas recent NMR studies indicate that this view is incorrect. Given the relevance of this discrepancy to P450 chemistry, it is important to determine whether Pdx favors the open or closed form of P450cam. Here, we have used both computational and experimental isothermal titration calorimetry studies that unequivocally show Pdx favors binding to the open form of P450cam. Analyses of molecular-dynamic trajectories also provide insights into intermediate conformational states that could be relevant to catalysis.

P450 | redox partner | conformation

Cytochrome P450, one of nature's largest enzyme families, is involved in a number of biological processes where monooxygenation is required. P450s are best known for their role in drug metabolism and clearance, steroid metabolism, the biosynthesis of numerous natural products, and the oxidative assimilation of various compounds as energy sources (1). P450s require additional protein redox partners that deliver electrons to the P450 heme iron, which is required for O_2 binding and activation (Fig. 1). A topic now receiving increasing attention is the effector role played by redox partner binding. In the well-studied cytochrome P450cam, redox partner binding results in P450 structural changes required for activity (2). The P450cam redox partner is putridaredoxin (Pdx), a Fe_2S_2 ferredoxin. It has been long known that P450cam is highly specific for Pdx because no other potential redox partner can support catalysis (3). Pdx delivers two electrons to P450cam (Fig. 1), and although any suitable low-potential reductant can deliver the first electron (step 1 in Fig. 1), the second electron-transfer step requires Pdx. It has been well established that Pdx binding results in changes in the spectral and physical properties of P450cam (3). For example, Pdx binding shifts P450cam from high to low spin (4), indicating that when Pdx binds, the active site opens up, thus allowing water to enter the active site and coordinate to the heme iron. Also consistent with opening of the active site is that Pdx binding destabilizes the P450cam–oxy complex ∼150-fold (5). Elegant double electron resonance (DEER) experiments (6) have also demonstrated that Pdx binding shifts P450cam from the closed to open state. Consistent with Pdx favoring the open form of P450cam, early NMR studies (7) determined that Pdx binding on the proximal face of P450cam results in structural changes on the opposite side of the protein that defines the substrate access channel. Finally, crystal structures of a covalently trapped P450cam–Pdx (8) and noncovalent complex (9) both show that P450cam adopts the open conformation in the presence of Pdx. Despite this large body of evidence supporting Pdx preferentially binding to the open form of P450cam, recent NMR studies led to the conclusion that Pdx binds to the closed form (10). That the open form was found in the crystal structures and DEER experiments was dismissed as artifacts of crystallization and the low temperature required for the DEER experiments. Given the relevance of Pdx-induced structural changes to understanding the relationship between redox partner binding and O_2 activation, it is important to rectify these discrepancies. As a step toward this goal, we have probed the energetics of Pdx binding to P450cam using both molecular dynamics (MD) simulations and direct binding assays. Consistent with a majority of the data available, we find that the open form of P450cam binds more tightly to Pdx than the closed form.

Results

As shown in Fig. S1, the trajectories of each individual component were well equilibrated within 40 ns as judged by the rms deviation of backbone atoms. As shown in Fig. 2, the buried surface area is substantially higher in the P450cam(O)–Pdx complex than in the P450cam(C)–Pdx complex. The P450cam(O)–Pdx complex results in the largest number of atom-to-atom contacts with an average of 33.64 atom-to-atom contact pairs per frame over the final 50 ns of the trajectory (*Methods*). The P450cam(C)–Pdx complex, conversely, has fewer contacts that were found to be stable over the trajectory, which results in fewer residues at the interface that were found to play a role in specific interfacial interactions as seen in Fig. 3, resulting in an average of 13.26 contact pairs over the final 50 ns. In addition, a critical intermolecular contact between Trp-106_{Pdx} and the C helix in P450cam is significantly weakened in in the P450cam(C)–Pdx complex. It has long been known that Trp-106_{Pdx} is critical for the effector role of Pdx (11). Tripathi et al. (8) postulated that Trp-106_{Pdx} is central to a Pdx-induced structural change in P450cam that is critical for arming the catalytic machinery required for proton-coupled electron transfer. In both the closed and open complex, $Trp106_{Pdx}$ forms tight nonbonded interactions with the C helix in P450cam. As shown in Fig. 3*A*, this interaction remains stable in in the crystal structure, but not in the NMR

Significance

Cytochrome P450 activates molecular oxygen to hydroxylate various molecules. This process requires the transfer of electrons from a redox partner, which further requires formation of a specific protein–protein complex. A question of increasing importance is whether or not the interaction between the P450 and its redox partner results in functionally important structural changes required for activity. The present work addresses the question of whether the redox partner favors binding to a specific conformer. This question is critically important in understanding how P450s activate molecular oxygen.

Author contributions: S.A.H. and D.B. designed research; S.A.H., D.B., and B.D.N. performed research; S.A.H., D.B., and T.L.P. analyzed data; and S.A.H., D.B., and T.L.P. wrote the paper.

The authors declare no conflict of interest.

This article is a PNAS Direct Submission.

[1]S.A.H and D.B contributed equally to this work.

[2]To whom correspondence should be addressed. Email: poulos@uci.edu.

This article contains supporting information online at www.pnas.org/lookup/suppl/doi:10.1073/pnas.1606474113/-/DCSupplemental.

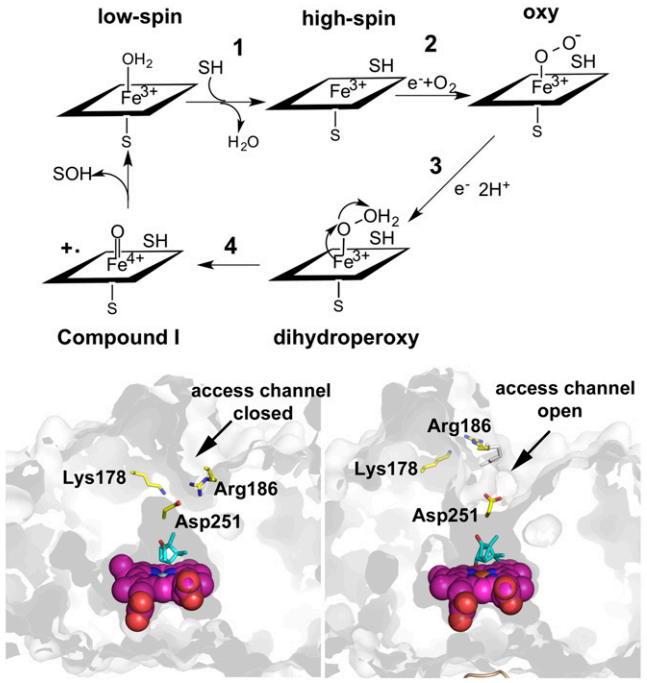

Fig. 1. Mechanism and conformational changes of P450cam. (*Upper*) The generalized cyclic mechanism of P450 substrate hydroxylation. After substrate binding, which displaces the water coordinated to the heme (step 1), an electron is transferred from putidaredoxin (Pdx) followed by binding of dioxygen (step 2). After a second electron transfer from Pdx and the addition of two protons (step 3), the system spontaneously forms the reactive compound I (step 4) that hydroxylates the substrate, which then leaves the active site. (*Lower*) In the closed state of P450cam (*Left*), Lys-178 and Arg-186 ion pairs with the catalytically important Asp-251, which closes the access channel from both substrates and solvent. In the open state (*Right*), these ion pairs are broken freeing Asp-251 to act in the proton relay network and opens the access channel through movements in F and G helices.

(Fig. 3*B*) structure. In the NMR structure, Pdx rotates about the Asp-38_{Pdx}–Arg-$112_{P450cam}$ ion pair resulting in Trp-106_{Pdx} sliding along the P450cam C helix, where it no longer forms any direct interactions with the backbone of the C helix after ∼30 ns into the simulation. This motion also results in a substantial movement of the C helix, which is required to maintain close contacts with Pdx. In sharp contrast, the C helix remains in place in the crystal structure. A comparison of the rms deviation of backbone atoms over the course of the simulation also shows that P450cam in the NMR structure experiences larger changes relative to the starting structure (Fig. S1). The one known critically important contact that remains intact in the NMR structure is the Asp-38_{Pdx}–Arg-$112_{P450cam}$ ion pair.

To further characterize the difference between these complexes, we used the molecular mechanics Poisson–Boltzmann solvent accessible (MM-PBSA) methodology to estimate relative free energies of interaction. The calculation was carried out for one snapshot every 100 ps over the course of the full simulations, which enables the calculation of SDs. The relative free energy of interaction (ΔG) between P450cam and Pdx is −60.2 ± 12.6 and −12.36 ± 15.0 kcal/mol for the crystal and NMR structures, respectively. The very large SD relative to the low interaction free energy in the NMR structure reflects a weaker and much less stable interface. These simulations indicate that Pdx favors binding to the open form of P450cam as found in the crystal structures and not the closed form of P450cam as observed in the NMR structure. If this is true, then direct binding measurements should give a lower K_D for Pdx binding to the open form of P450cam than the closed form. We chose isothermal titration calorimetry (ITC) as the best approach for comparing K_D for three reasons. First, ITC does not necessitate modification of the proteins for immobilization or the addition of fluorogenic tags, which is required for other methods like surface plasmon resonance or microscale thermophoresis, respectively. Second, it already has been shown that ITC is a useful method for measuring the P450cam–Pdx interaction and P450cam–Pdx binding is dominated by a large enthalpy (12) change so the signal is large. Third, the latest generation of ITC instrumentation requires far less sample and time for accurate measurements than other similar methods would demand.

Direct Binding Assays. Our ITC results are summarized in Fig. 4. In the absence of substrate (the open form of P450cam), the measured K_D is 19.4 ±1.23 μM, whereas in the presence of camphor (the closed state) the K_D was determined to be 44.6 ± 2.97 μM. Replication of these experiments gave values of 13.4 ± 2.0 and 43.4 ± 2.97 μM for the substrate-free and -bound forms, respectively. Another indication that substrate-free binds more tightly to Pdx is that the binding curve of the substrate-free P450cam exhibits greater sigmoidicity and saturates at lower Pdx concentrations than the substrate-bound form. As observed in earlier ITC experiments (12), the reaction is enthalpically driven, most likely because of the formation of intermolecular ion pairs and H-bonds between P450cam and Pdx. These results clearly demonstrate that Pdx forms a more stable complex with the open, substrate-free form of P450cam. This finding is consistent with not only the MD-derived results, but also the crystal structures (8, 9), DEER experiments (6), the shift of P450cam to the low-spin (more open) state when Pdx binds (4), and the large decrease in stability of the P450cam–oxy complex in the presence of Pdx (3, 5).

Relevance to Catalysis. It has traditionally been thought that the closed form of P450cam with the substrate-binding pocket sequestered from solvent must be the most active form of the enzyme. However, when considering that Pdx binding is required for activity and Pdx favors the open form of P450cam, one could logically conclude that the more open state is the most active form. Because Pdx exerts its effector role on the second electron-transfer step, it was concluded by Tripathi et al. (8) that the switch to the open form is associated with activation of the proton-coupled electron transfer system (step 3 in Fig. 1). Central to this

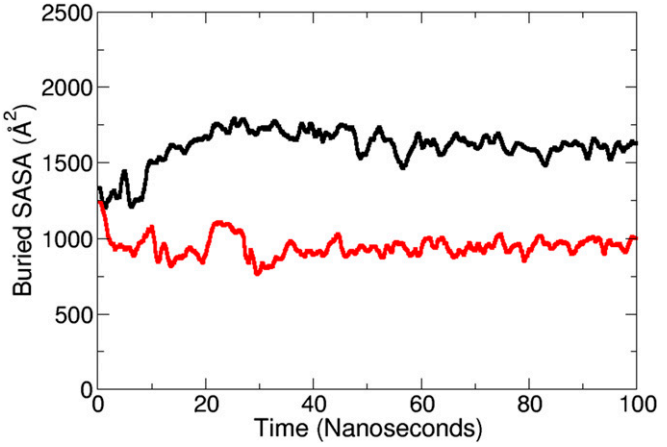

Fig. 2. Calculated buried surface area in the P450cam-Pdx complexes. Buried solvent-accessible surface area (SASA) was calculated by calculating the sum of the surface areas of P450cam and Pdx separately then subtracting the surface area of the P450cam–Pdx complex for the P450cam(O)–Pdx (black line) and P450cam(C)–Pdx (red) systems over the full 100-ns trajectory using a running average of 100 ps.

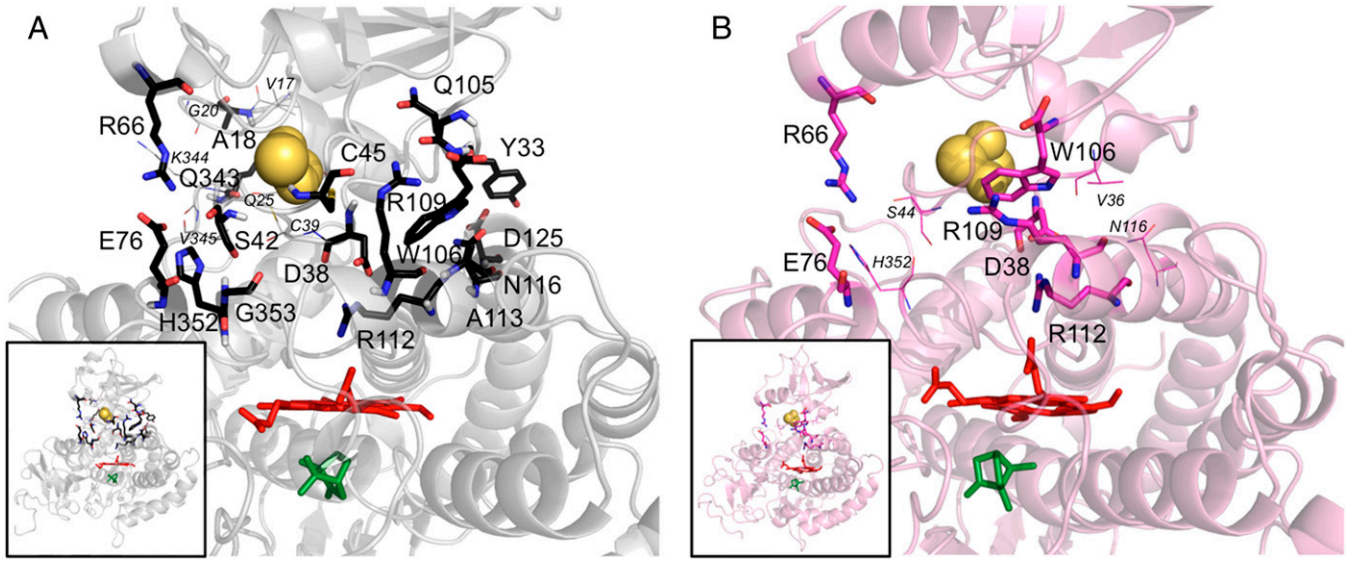

Fig. 3. Comparisons of the interfaces of the equilibrated P450cam-Pdx complexes by MD. The interface of P450cam–Pdx complexes are shown for the P450cam(O)–Pdx (*A*) and P450cam(C)–Pdx (*B*) systems after equilibration by MD simulation. For each system, the iron sulfur cluster is shown as yellow spheres, the heme (and O_2 for the oxy complex) in red sticks, and camphor in green sticks for reference. Interfacial residues that were found to average at least one atom-to-atom contact of 3.5 Å or less per frame over the full 100 ns (or termed strong contacts; *Methods*) are shown as thick sticks and labeled with larger residue numbers, whereas those residues that were found to average between 0.5 and 0.999 pairs per frame (those residues that play smaller roles at the interface) are shown as thin sticks and are labeled using smaller numbers in italic. See *Methods* for more details on the calculation of contact pairs.

hypothesis is the highly conserved Asp-251 (Fig. 1), which is known to be essential for activity. Asp-251 is thought to be involved in a proton relay network required for proper protonation of the iron-linked dioxygen in the oxy complex (13, 14), resulting in heterolytic cleavage of the O–O bond and formation of the reactive compound I. In the closed form, however, Asp-251 is tied up with salt bridges to Arg-186 and Lys-178 (Fig. 1). When Pdx binds, however, the active site opens up, these salt bridges are broken, and Asp-251 now is free to serve its catalytic function (Fig. 1). Relevant to this postulated Asp-switch mechanism is that in the P450cam–Pdx crystals that were grown in the presence of excess camphor, the product 5-*exo*-hydroxycamphor is bound at the active site, whereas in the many datasets reported for P450cam in the closed form, only camphor has been observed in the active site. This finding strongly suggests that X-ray–generated reducing equivalents can drive substrate hydroxylation in the open form of P450cam, but not the closed form.

One problem with this view, however, is that in the open form the loosening of protein–substrate contacts could lead to orientational disorder of the substrate and the loss of regioselective hydroxylation. Our MD simulations of the open and closed forms of P450cam in the absence of Pdx provide some insight into this

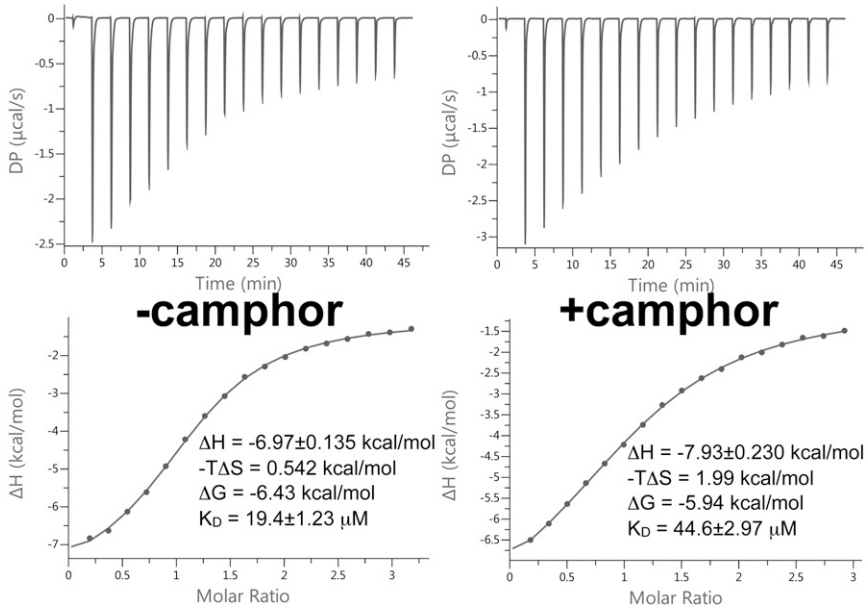

Fig. 4. ITC of P450cam in the presence and absence of substrate, D-camphor. Experimental details are provided in *Methods*. Data were fit by using MicroCal PEAQ-ITC software. Based on the best fits, the total number of binding sites is 1.13 ± 0.001 in the absence of camphor and 1.12 ± 0.001 in the presence of camphor.

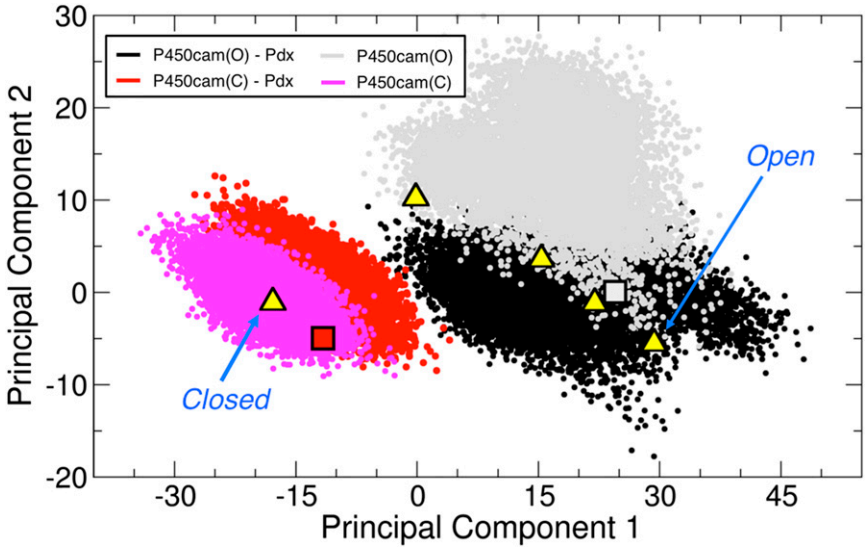

Fig. 5. Conformational dynamics of P450cam in differing conformational and complex states. PCA was used to project the conformational dynamics of P450cam onto principal component space every 10 ps over the full 100-ns trajectory for each of the six systems that included P450cam. The boxes overlaid onto the plot designate the simulation starting points after minimization; P450cam(O)–Pdx and P450cam(O), (24.47, 0.06); and P450cam(C)–Pdx and P450cam (C), (−11.66, −4.95). In an effort to provide points of reference in principal component space, five crystal structures are also labeled as yellow triangles; 5CP4 (P450cam in a closed conformation), (−17.84, −1.07); 3P6X (P450cam in the most open conformation observed), (29.30, −5.51); and three additional intermediates solved (PDB ID codes 1RE9, 1RF9, and 3P6T) that used tethered substrates to trap intermediated between open and closed at (−0.16, 10.23), (15.38, 3.61), and (21.96, −1.14), respectively, similar to the mapping performed by Markwick et al. (19).

possibility. The fraction of time the correct carbon spends near the Fe atom relative to the other camphor carbon atoms is the simplest way to compare the possible loss or retention of regioselectivity. Normally, with P450cam the C4-Fe distance is not included because this is the least reactive carbon (15). In the closed form, the distance between the camphor atom to be hydroxylated, C5, and the heme iron remains < 4.5 Å 84% of the time over a 100-ns simulation. The next closest atom (C9), one of the gem–dimethyl carbons, spends 10% of the time within 4.5 Å of the iron. In sharp contrast, the camphor remains in this orientation only 25% of the time in the open conformation, whereas the next nearest carbon atom (also C9) spent a 35% of time within 4.5 Å of the iron. We also carried out a control simulation with another P450, CYP101D1. CYP101D1 is a very close homolog to P450cam, with an rms deviation of 1.0 Å for backbone atoms and has a very similar active site structure (16). CYP101D1 catalyzes exactly the same reaction as P450cam at the same rate giving the same single product (16). However, CYP101D1 is more promiscuous, with respect to redox partner selectivity because Pdx can support CYP101D1 catalysis despite not being its natural redox partner (17). In addition, the natural CYP101D1 Fe_2S_2 redox partner does not shift CYP101D1 more toward the low-spin state. With CYP101D1 in the closed substrate-bound form, C5 spends 45% of the time within 4.5 Å of the iron, with the next closest atom (once again C9) spending 24% of the time within 4.5 Å of the iron. Therefore, substrate tumbling in the closed form of CYP101D1 is in between closed and open P450cam, yet CYP101D1 gives only one product. We also note that the next closest camphor atom to the iron in all three simulations is C9. Given that the heat of formation of the C9 radical is ∼1 kcal/mol less favorable than the C5 radical (15), C5 hydroxylation will be slightly preferred.

Although this analysis could be interpreted as the open form being compatible with regioselective hydroxylation, it also is possible that in the P450cam–Pdx crystals, X-ray–driven reduction and regioselective hydroxylation is observed, owing to the cryogenic temperatures required for data collection. In effect, the substrate is "frozen" in place and locked down into a relatively shallow energy minimum. We therefore consider the possibility that P450cam need not adopt the totally open state, but that the minimum structural change required for activity is loosening the Asp-251 salt bridges in order for the proton relay network to be established, while maintaining tight protein–substrate contacts. This situation further suggests that the active conformer may be somewhere between the totally open and closed states. Relevant to this analysis are the several crystal structures solved by Lee et al. (18), where P450cam was trapped in the partially open state using substrates with longer tethers that extend through the substrate access channel. In some of these intermediate structures, the Asp-251 salt bridges are broken, but the active site does not completely open, and tight substrate contacts are maintained.

Principal component analysis (PCA) of MD trajectories is another method for sampling conformational space and can provide insight into partially populated conformational states relevant to catalysis. We therefore carried out PCA on P450cam in the P450cam–Pdx complex in both the closed and open states, in addition to P450cam in the absence of Pdx in both the open and closed states (Fig. 5). Previous work by Markwick et al. (19) helped map out principal component space for P450cam using the first two principal components, and our PCA analysis of P450cam displays good agreement with their previous mapping using the identical set of previously solved P450cam crystal structures of the partially open states (Fig. 5, yellow triangles) (18, 19). The closed form of P450cam in the absence of Pdx (Fig. 5, magenta) samples broadly around (−15, −1.0), whereas the presence of Pdx in the P450cam(C)–Pdx complex (Fig. 5, red) appears to only shift the center of the distribution to (−9.0, −1.0). This population shift is toward the open form of P450cam, which in the absence of Pdx (Fig. 5, gray) samples broadly around (18.0, 15.0). Importantly, however, neither in the absence nor presence of Pdx was the closed state ever observed to shift fully to the open state, consistent with the classical MD results of Markwick et al. (19).

The distributions of conformational sampling of P450cam in the open form in the presence and absence of Pdx are also distinctly different. The open form of P450cam samples a large region centered around (18.0, 15.0), whereas in the presence of Pdx (Fig. 5, black), the distribution is centered near (20, 0). Similar to the

closed form analysis above, neither in the presence nor absence of Pdx was the open form observed to shift to the closed state. Of particular interest, however, are the locations of the intermediate-open conformations that have been experimentally observed in ref. 18 (Fig. 5, yellow triangles). The distribution of the open form of P450cam in the P450cam(O)–Pdx complex better samples the conformations of these intermediate-open structures than P450cam(O) alone, suggesting that Pdx may act in aiding P450cam in sampling these intermediate states between the closed and open states that have been previously observed by crystallography.

Conclusions

Consistent with a wealth of published work, this study demonstrates that Pdx favors binding to the open form of P450cam. Therefore, that two crystal structures (8, 9) and DEER experiments (6) showing that P450cam adopts the open state when bound to Pdx is not, as previously claimed (10), an artifact of crystallization or the cryogenic temperatures required for these experiments. Still open for debate, however, is which form of P450cam is the active form. That the stable lowest-energy state observed in solution and in crystals is the open form does not necessarily mean it is the active form. For the Asp-switch mechanism to operate, all that is necessary is a loosening of the Asp-251 salt bridges, which may not require a complete shift from closed to open. Conversely, there is nothing inconsistent with an open active site, resulting in highly coupled P450 chemistry and regioselective hydroxylation. The best example here is nitric oxide synthase (NOS). NOS operates like a typical P450 in the hydroxylation of its substrate, L-Arg, and, like P450cam, NOS is both highly specific and coupled, yet in NOS the active site is always open and exposed to solvent. The key to specific and efficient substrate hydroxylation is holding the substrate in the correct orientation and efficient delivery of protons to dioxygen. Because this requirement can be achieved in NOS with an open active site, then P450s should be able to do the same. The main reason for considering that some intermediate state might be the active form in P450cam is that tight substrate–protein interactions may be too loose in the totally open form to ensure regioselective hydroxylation. In addition to the PCAs presented here and in previous publications (19), and the several crystal structures of P450cam (18) in states between the open and closed forms, these results indicate that a potentially active intermediate state is sufficiently populated with a long enough lifetime to accommodate the much faster proton-coupled electron transfer processes required for regioselective and stereoselective substrate hydroxylation.

Methods

MD. MD simulations were used to compare the stability of the P450cam–Pdx complex when P450cam is in the open and closed state, P450cam(O) and P450cam(C), respectively. The starting structure for the P450cam(O)–Pdx system was the crystal structure solved by Tripathi et al. (8) with the cross-linker removed and the system mutated to wild type (8), identical to the starting point used in our previous MD study (20). For P450cam(C)–Pdx simulations, we started with the published NMR structure of Pdx in complex with P450cam in the ferric, closed state (PDB ID code 2M56) (9). These complex systems were placed in orthogonal unit cells with a 10-Å cushion around the complex, resulting in the addition of 18,981 and 18,070 water molecules for the P450(O)–Pdx and P450(C)–Pdx complexes, respectively. Each system was then neutralized through the addition of sodium ions. The resulting open and closed P450cam–Pdx complex systems consisted of a total of 65,005 and 63,895 atoms, respectively. As controls, we also carried out simulations of the open and closed forms of P450cam in the absence of Pdx, as well as Pdx in the absence of P450cam. We also included CYP101D1 (PDB ID code 4C9K) (17) as a control. CYP101D1 is a very close homolog to P450cam and uses camphor as a substrate to give the same product as P450cam (16). Comparing CYP101D1 with P450cam provided insights on the range of motion that the substrate can experience, yet retain regioselective and stereoselective hydroxylation.

Simulations for all classic MD simulations were carried out with the Amber 12 simulation package (21). The parameters used here were identical to those used in a previous study (20), but are discussed briefly here. The ff10 force fields were used to model protein, whereas the Cys-heme ligand parameters were taken from Shahokh et al. (22). The parameters for the Fe_2S_2 iron–sulfur cluster were taken from ref. 23, and parameters for the substrate camphor were derived from antechamber with the gaff forcefield (24) by using the bond charge correction charging scheme (25). The TIP3P water model was used to model the water in each simulation, and counterions were added to achieve a net neutral charge for each system.

Each structure was prepared for MD simulation by first carrying out 1,000 cycles of energy minimization, with all heavy atoms except water molecules held fixed in position, followed by an additional 1,000 cycles where the fixed restraints were removed. Production runs for each system were completed with a 1-fs time step, with coordinates saved every 10 ps for analysis. The temperature and pressure were held constant through weak coupling with a 1-ps pressure relaxation time and Langevin dynamics using a collision frequency of 1 ps^{-1}. Periodic boundary conditions were used and electrostatic interactions were calculated with a Particle Mesh Ewald implementation of the Ewald sum (26). A spherical cut-off of 10.0 Å was used for the calculation of nonbonded interactions, and bonds involving hydrogen atoms were constrained by using SETTLE (27).

Analysis of the resulting trajectories was carried out by using the Amber software suite (21), VMD (28), the Bio3D R package (29, 30), and locally developed analysis tools. Buried surface area over the course of each complex trajectory was calculated by subtracting the solvent-accessible surface area of the full complex as calculated by VMD using a probe radius of 1.4 Å from the combined surface areas of P450cam and Pdx separately. Analysis of the interface contacts was carried out by using locally developed analysis tools that have previously been used to document major atom-to-atom contacts (20), but is briefly described here. For every frame of a given trajectory, atom-to-atom contact pairs are recorded for every atom-to-atom pair that is within 3.5 Å. The resulting contacts are then summed up over the full trajectory and further summarized by residue to produce a list of the number of residue-to-residue contacts over the full trajectory. To aid in designating the staying power of the contact over the full trajectory, each sum is then divided by the number of frames where cut-offs of $\geq$1.0 atom-to-atom contact per frame are designated as major contacts, whereas $1.0 > x \geq 0.5$ contacts are designated as a minor contact. Finally, MM-PBSA energy calculations for the complexes used the single trajectory method for calculating the energies for Pdx, P450cam, and the complex itself from the complex trajectory (31, 32), as described both in the Amber manual and in ref. 32.

ITC. All experiments were performed with the MicroCal PEAQ-ITC instrument from Malvern. P450cam and Pdx used for the experiments were overexpressed and purified from *Escherichia coli* using described methods (33). The 50 mM phosphate buffer at pH 7.4 was used for all experiments. For experiments in the presence of camphor, a final concentration of 1 mM D-camphor was used. DTT or any other reducing agents were removed from both protein preparations before experiments. All experiments were performed at 25 °C, with the reaction cell containing 300 μL of 100 μM P450cam, and the injection syringe was filled with 1.75 mM Pdx.

Each titration experiment was performed by using 18 injections of 2 μL with 4-s duration and a 150-s interval between injections. Reference power of 5, high-feedback mode, and a stirring speed of 750 rpm were used for all experiments. All data were analyzed by using the MicroCal PEAQ-ITC analysis software. To obtain the binding enthalpies, the observed enthalpy values were corrected for the enthalpy of dilution obtained under identical conditions with the sample cell containing buffer alone.

ACKNOWLEDGMENTS. We thank Drs. Douglas Tobias and David Mobley for many thoughtful discussions during the duration of this study; and Nubwwe Beach and Verna Frasca from Malvern Instruments for assistance with analysis of the ITC data. This research was supported by an institutional Chemical and Structural Biology Training Grant Predoctoral Fellowship T32-GM10856 (to S.A.H.) and NIH Grant GM57353 (to T.L.P.). Simulation time was provided in part by XSEDE Allocation TG-MCB130001 (to S.A.H. and T.L.P.).

1. Ortiz de Montellano P, ed (2015) *Cytochrome P450: Structure, Mechanism, and Biochemistry* (Springer, New York).
2. Poulos TL (2014) Heme enzyme structure and function. *Chem Rev* 114(7): 3919–3962.
3. Lipscomb JD, Sligar SG, Namtvedt MJ, Gunsalus IC (1976) Autooxidation and hydroxylation reactions of oxygenated cytochrome P-450cam. *J Biol Chem* 251(4):1116–1124.
4. Unno M, et al. (1997) Resonance Raman investigations of cytochrome P450(cam) complexed with putidaredoxin. *J Am Chem Soc* 119:6614–6620.

5. Glascock MC, Ballou DP, Dawson JH (2005) Direct observation of a novel perturbed oxyferrous catalytic intermediate during reduced putidaredoxin-initiated turnover of cytochrome P-450-CAM: Probing the effector role of putidaredoxin in catalysis. *J Biol Chem* 280(51):42134–42141.
6. Myers WK, Lee YT, Britt RD, Goodin DB (2013) The conformation of P450cam in complex with putidaredoxin is dependent on oxidation state. *J Am Chem Soc* 135(32): 11732–11735.
7. Pochapsky SS, Pochapsky TC, Wei JW (2003) A model for effector activity in a highly specific biological electron transfer complex: The cytochrome P450(cam)-putidaredoxin couple. *Biochemistry* 42(19):5649–5656.
8. Tripathi S, Li H, Poulos TL (2013) Structural basis for effector control and redox partner recognition in cytochrome P450. *Science* 340(6137):1227–1230.
9. Hiruma Y, et al. (2013) The structure of the cytochrome p450cam-putidaredoxin complex determined by paramagnetic NMR spectroscopy and crystallography. *J Mol Biol* 425(22):4353–4365.
10. Skinner SP, et al. (2015) Delicate conformational balance of the redox enzyme cytochrome P450cam. *Proc Natl Acad Sci USA* 112(29):9022–9027.
11. Sligar SG, Debrunner PG, Lipscomb JD, Namtvedt MJ, Gunsalus IC (1974) A role of the putidaredoxin COOH-terminus in P-450cam (cytochrome m) hydroxylations. *Proc Natl Acad Sci USA* 71(10):3906–3910.
12. Aoki M, Ishimori K, Fukada H, Takahashi K, Morishima I (1998) Isothermal titration calorimetric studies on the associations of putidaredoxin to NADH-putidaredoxin reductase and P450cam. *Biochim Biophys Acta* 1384(1):180–188.
13. Gerber NC, Sligar SG (1994) A role for Asp-251 in cytochrome P-450cam oxygen activation. *J Biol Chem* 269(6):4260–4266.
14. Vidakovic M, Sligar SG, Li H, Poulos TL (1998) Understanding the role of the essential Asp251 in cytochrome p450cam using site-directed mutagenesis, crystallography, and kinetic solvent isotope effect. *Biochemistry* 37(26):9211–9219.
15. Collins JR, Loew GH (1988) Theoretical study of the product specificity in the hydroxylation of camphor, norcamphor, 5,5-difluorocamphor, and pericyclocamphanone by cytochrome P-450cam. *J Biol Chem* 263(7):3164–3170.
16. Yang W, et al. (2010) Molecular characterization of a class I P450 electron transfer system from *Novosphingobium aromaticivorans* DSM12444. *J Biol Chem* 285(35): 27372–27384.
17. Batabyal D, Poulos TL (2013) Crystal structures and functional characterization of wild-type CYP101D1 and its active site mutants. *Biochemistry* 52(49):8898–8906.
18. Lee YT, Wilson RF, Rupniewski I, Goodin DB (2010) P450cam visits an open conformation in the absence of substrate. *Biochemistry* 49(16):3412–3419.
19. Markwick PRL, Pierce LCT, Goodin DB, McCammon JA (2011) Adaptive accelerated molecular dynamics (Ad-AMD) revealing the molecular plasticity of P450cam. *J Phys Chem Lett* 2(3):158–164.
20. Hollingsworth SA, Poulos TL (2015) Molecular dynamics of the P450cam-Pdx complex reveals complex stability and novel interface contacts. *Protein Sci* 24(1):49–57.
21. Case DA, et al. (2005) The Amber biomolecular simulation programs. *J Comput Chem* 26(16):1668–1688.
22. Shahrokh K, Orendt A, Yost GS, Cheatham TE, 3rd (2012) Quantum mechanically derived AMBER-compatible heme parameters for various states of the cytochrome P450 catalytic cycle. *J Comput Chem* 33(2):119–133.
23. Chang CH, Kim K (2009) Density functional theory calculation of bonding and charge parameters for molecular dynamics studies on [FeFe] hydrogenases. *J Chem Theory Comput* 5(4):1137–1145.
24. Wang J, Wolf RM, Caldwell JW, Kollman PA, Case DA (2004) Development and testing of a general amber force field. *J Comput Chem* 25(9):1157–1174.
25. Jakalian A, Jack DB, Bayly CI (2002) Fast, efficient generation of high-quality atomic charges. AM1-BCC model: II. Parameterization and validation. *J Comput Chem* 23(16): 1623–1641.
26. Darden T, Perera L, Li L, Pedersen L (1999) New tricks for modelers from the crystallography toolkit: The particle mesh Ewald algorithm and its use in nucleic acid simulations. *Structure* 7(3):R55–R60.
27. Miyamoto S, Kollman PA (1992) SETTLE: An analytical version of the SHAKE and RATTLE algorithm for rigid water molecules. *J Comput Chem* 13:952–962.
28. Humphrey W, Dalke A, Schulten K (1996) VMD: Visual molecular dynamics. *J Mol Graph* 14(1):33–38.
29. Grant BJ, Rodrigues AP, ElSawy KM, McCammon JA, Caves LS (2006) Bio3d: An R package for the comparative analysis of protein structures. *Bioinformatics* 22(21): 2695–2696.
30. Skjærven L, Yao XQ, Scarabelli G, Grant BJ (2014) Integrating protein structural dynamics and evolutionary analysis with Bio3D. *BMC Bioinformatics* 15:399.
31. Massova I, Kollman PA (2000) Combined molecular mechanical and continuum solvent approach (MM-PBSA/GBSA) to predict ligand binding. *Perspect Drug Discov Design* 18(1): 113–135.
32. Gohlke H, Case DA (2004) Converging free energy estimates: MM-PB(GB)SA studies on the protein-protein complex Ras-Raf. *J Comput Chem* 25(2):238–250.
33. Sevrioukova IF, Garcia C, Li H, Bhaskar B, Poulos TL (2003) Crystal structure of putidaredoxin, the [2Fe-2S] component of the P450cam monooxygenase system from *Pseudomonas putida*. *J Mol Biol* 333(2):377–392.